Construction and Building Materials 26 (2012) 723–729

Contents lists available at ScienceDirect

Construction and Building Materials

journal homepage: www.elsevier.com/locate/conbuildmat

Threshold chloride level and characteristics of reinforcement corrosion initiation in simulated concrete pore solutions

Hui Yu [a], Kuang-Tsan K. Chiang [b,*], Lietai Yang [b]

[a] Materials Engineering Department, Mechanical Engineering Division, Southwest Research Institute®, 6220 Culebra Road, San Antonio, TX 78238, USA
[b] Department of Earth, Material, and Planetary Sciences, Geosciences and Engineering Division, Southwest Research Institute®, 6220 Culebra Road, San Antonio, TX 78238, USA

ARTICLE INFO

Article history:
Received 6 April 2011
Received in revised form 21 June 2011
Accepted 23 June 2011
Available online 23 July 2011

Keywords:
Threshold chloride level (C_{th})
Reinforced steel bar (rebar)
Corrosion initiation
Simulated concrete pore solution (SPS)
Open circuit potential (OCP)
Linear polarization resistance (LPR)
Corrosion current density (i_{corr})
Potentiodynamic polarization

ABSTRACT

Threshold chloride level (C_{th}) and corrosion behavior of reinforced steel bar (rebar) have been studied in three kinds of simulated concrete pore solutions (SPSs). The rebars with two different surface conditions were immersed in SPSs and open circuit potential (OCP) and linear polarization resistance (LPR) were monitored with stepwise chloride addition. Different electrochemical techniques for C_{th}s and rebar corrosion initiation of all cases are discussed and compared with results from the literature. The results indicate that C_{th}s acquired from both OCP and LPR techniques are relatively consistent. C_{th}s, represented by the threshold expression $[Cl^-]$ or $[Cl^-]/[OH^-]$, exhibit an increasing trend with increasing SPS pH. Corrosion resistance of both sandblasted and prerusted bars can be improved by raising the pH of the SPS solution; the extent of improvement is more pronounced for sandblasted bars. Once initiated, severe pit corrosion occurs on sandblasted bars with more abrupt OCP and corrosion current density variation exhibited.

1. Introduction

Chloride-induced corrosion of reinforced steel bar (rebar) is one of the major causes of premature degradation of reinforced concrete and consequent structure collapse [1]. Chlorides, from either the marine environment or deicing salt applications, can compromise rebar passivity and initiate active corrosion once the chloride content at the rebar surface reaches a threshold level (C_{th}) [2]. Once corrosion occurs, the process is nonreversible and may lead to concrete structure cracking and spallation. Thus, it is critical to determine C_{th} and understand the characteristics of reinforcement corrosion initiation.

Recently, several sources [3–6] summarized historical data of C_{th}s inducing rebar corrosion initiation in concrete. These data revealed that the reported C_{th}s vary by more than one order of magnitude (chloride varies from 0.2% to 3.04% on a cement weight basis or 0.8–12.16 kg/m^3 concrete, assuming 400 kg/m^3 cement content). C_{th} values are scattered because they are acquired based on factors such as varying rebar surface status, corrosion initiation determination techniques, and exposure environments, which are generally considered the most crucial factors affecting C_{th} determination.

Paste, mortar, and concrete with embedded rebar have been used to investigate corrosion issues in the laboratory. However, such investigation is time consuming even though diverse measures are used to speed up chloride migration into solid blocks and reach C_{th} [7,8] at the rebar surface. Decades ago, researchers [9–11] originally use simulated concrete pore solutions (SPSs) as an alternative media to characterize rebar corrosion initiation. Although studies with SPSs cannot capture the whole C_{th} spread that occurs in concrete, SPS is still widely adopted as a substitute of concrete to rapidly evaluate various rebar materials and the effect of corrosion inhibitors [10,12–16]. Also, several SPSs were defined to represent variable concrete pore water components. Hurley and Scully [12] once compared reported C_{th} data achieved from SPSs with those acquired from mortar or concrete. Results indicated that the latter are greater than the former. This may be attributable to chloride binding in cementitious materials and the interface conditions existing between rebar/mortar or concrete, in which a lime-rich layer not only acts as a physical barrier but also buffers the action of chloride activity [13]; homogenous SPSs cannot provide this inhibition function. Nevertheless, SPSs as optional media to investigate corrosion issues of reinforcement in the laboratory are still adopted widely [10,14–16].

C_{th} is generally expressed as total chloride content (the total chloride content as a percentage by weight of cement or concrete) or $[Cl^-]/[OH^-]$ ratio. Merits of the former expression are that it is

* Corresponding author. Tel.: +1 210 522 2308; fax: +1 210 522 5184.
E-mail address: kchiang@swri.org (K.-T. K. Chiang).

0950-0618/$ - see front matter © 2011 Elsevier Ltd. All rights reserved.
doi:10.1016/j.conbuildmat.2011.06.079

relatively easy to measure and includes the corrosion risk of bound chloride and the inhibitive effect of cement hydration products. Ann and Song [5] illustrated that total chloride is a better expression for C_{th} because all free chloride and most bound chloride participate in rebar corrosion initiation, especially at low pH. The expression of $[Cl^-]/[OH^-]$ reflects the ratio of aggressive to inhibitive ions causing corrosion initiation in a solution environment. The following equation is generally used to describe the relationship between chloride threshold and hydroxyl ions [8]:

$$pH = n \times \log Cl^- + k \quad (1)$$

where n and k are constants with n being approximately 0.8. This implies that the ratio $[Cl^-]^{0.8}/[OH^-]$ would be a constant for corrosion occurrence. In some literature, the corrosion initiation criterion is also defined as a $[Cl^-]/[OH^-]$ ratio greater than 0.6 [17]. Thus, it is feasible to achieve a defined value or a narrow range of this ratio in SPS because the reported data are relatively consistent. However, the $[Cl^-]/[OH^-]$ ratio does not consider the dependence of chloride binding capacity on the hydroxyl concentration. Additionally, an increase in the pH above 12.6 has been observed to produce a decrease in the level of bound chloride, indicating that an increase in corrosion risk accompanies an increase in hydroxyl ions, in spite of the inhibitive effect of hydroxyl ion [18].

Rebar surface condition has been shown to be a critical factor for corrosion initiation [19]. In the laboratory, the reinforcing steel is usually pretreated prior to testing (e.g., by sandblasting or polishing), whereas in field applications, the reinforcement is used as-received and might be prerusted or covered with mill scale. Mohammed and Hamada [20] investigated corrosion resistance of rebars, with various surface conditions, covered with cement paste (prepassivated) before casting. The rank of corrosion resistance is prepassivated > black-rusted > polished > brown rusted > mill scaled bars. Manera et al. [21] also revealed that the C_{th} acquired for a polished steel surface is higher than that for as-received steel both in SPS and in concrete slabs.

Electrochemical approaches have been widely deployed for determining rebar corrosion initiation and extent, qualitatively and quantitatively, for several decades. Half-cell potential (open circuit potential, OCP) measurement for rebar corrosion initiation determination is sensitive and convenient and has been standardized [22]. In this case, an absolute OCP value or an abrupt potential negative shift is generally used as a criterion of rebar corrosion initiation. However, there are controversial experimental results [23] with the absolute OCP value criterion. These results indicate that this criterion is not unconditional because the measured OCP values are also oxygen or IR (current × resistance) drop related, which makes it difficult to accurately define this criterion. In addition, an apparent drawback for OCP measurement is that it cannot quantitatively express the extent of rebar corrosion. Thus, OCP that drops apparently and does not recover in a continuous measurement period is generally used as a rebar corrosion initiation criterion in the laboratory. Another nondestructive technique, linear polarization resistance (LPR), is also used to characterize corrosion initiation and propagation according to a defined criterion value of corrosion current density, i_{corr}, or the abrupt variation of i_{corr}. Generally, when the i_{corr} is greater than 0.1 μA/cm^2, the rebar is considered corroded. Similarly, as the criterion of absolute OCP value, 0.1 μA/cm^2 is not an unconditional value, because it is difficult to specify rebar surface area and constants in calculations. However, the relatively sharp variation of i_{corr} can effectively minimize the errors mentioned previously and can be a better indicator for rebar corrosion initiation.

Li and Sagûës [24–27] have systematically studied C_{th} for variable rebar surface status (i.e., including sandblasted, as-received and minor pre-rusted) in high pH SPSs, including SPS2 (pH = 13.6), SPS1 (pH = 13.3), and saturated calcium hydroxide ($Ca[OH]_2$; SCS) (pH = 12.6) with electrochemical techniques such as OCP, electrochemical impedance spectroscopy (EIS), and cyclic polarization. The results indicate that (1) C_{th} in SPSs depends strongly on pH and when pH reaches 13.6, active corrosion cannot be sustained until $[Cl^-]$ is very high and (2) one main cause of the large scatter in the reported C_{th} results is the variability of concrete pore water pH and chloride binding ability. However, it is necessary to further confirm these conclusions with extended pH range and correlate the results acquired from different approaches.

In this paper, C_{th}, represented with $[Cl^-]$ and $[Cl^-]/[OH^-]$, for sandblasted and prerusted bars in three different pH SPSs is investigated with OCP and LPR techniques. Electrochemical characteristics of rebar corrosion initiation, including variations of OCP and i_{corr}, with both bar surface conditions are also addressed.

2. Experiment

2.1. Specimen preparation

Approximately 200-mm-long samples were cut from ordinary A-615 reinforcing steel bar (size: approximately 10 mm in diameter). The chemical composition of the bar is presented in Table 1. Prior to test exposure, half of the specimens were sandblasted to remove mill scales and rust. The other half were put into an environmental chamber, in which Florida coast high temperature and salty humidity atmosphere were simulated, for 6 days to produce a thick rust layer on the bar surface. Subsequent to the salt-fog environment exposure, the prerusted bars were carefully cleaned with distilled water to avoid contamination of the SPSs in the test cell by chloride in the rust layer. Photographs of the specimens are shown in Fig. 1a. The specimens were drilled and tapped at one end for electrical connection. The specimens were covered with epoxy on both ends, and approximately 24 cm^2 of the surface was exposed for the experiment.

2.2. Experimental setup

A 2 L glass container was used as a test cell in this study. Three types of SPSs were selected as pore water solutions. The chemical compositions of the SPSs are presented in Table 2. The lower pH (SPS4) solution was intended to present pore water within a carbonated concrete environment. Approximately 1.5 L SPS was used in each glass container and its pH was monitored throughout the experiment. Because the results of deviation were less than 0.1, the effects on experimental results induced by pH fluctuation were ignored. Chloride concentration in SPSs was adjusted stepwise by adding reagent-grade NaCl crystals. For the chloride adjusting process, approximately 100 mL solution was extracted with a syringe from the test cell. After the NaCl crystals dissolved completely, the extracted solution was poured back into the cell. A magnetic stirring bar was placed at the bottom of each container and was set to rotate at the lowest rate to continuously mix the solution homogeneously throughout the experiment, including the duration when the electrochemical measurements (see below) were conducted. Ambient temperature was held at 23 ± 2 °C. To reduce carbonation, all cells were covered except during NaCl crystal addition and pH monitoring. At the beginning of the experiment, the specimens were immersed in designated SPS 2 days for preconditioning. Subsequently, chloride was adjusted and the interval for the chloride stepwise increment was approximately 3 days. OCP data were automatically and continuously recorded by a multichannel Gamry Potentiostat (Electrochemical Multiplexer ECMB) at 30-min intervals. The data of the first 24 h after each NaCl increment were not recorded, because the solution may be heterogeneous and erroneous data produced.

Two specimens, one with a sandblasted surface and the other severely prerusted, were immersed in SPS in one cell. A 12 × 30-cm titanium mesh was embedded in the cell as a counter-electrode for LPR measurements. A saturated calomel electrode (SCE) was inserted into each cell as a reference electrode. The SCE was packed with porous zirconium frit to avoid contamination induced by long-term contact with high alkalinity SPSs. Also, the SCE was calibrated with standard reference and the calibration was periodically checked during NaCl adjustment. The experimental setup is shown in Fig. 1b.

Prior to each stepwise NaCl adjustment, LPR measurements were performed with the same potentiostat. The scan rate was 0.1667 mV/s and the polarizations range was ±14 mV vs. rebar OCP. The polarization resistance, R_p, is equal to the slope of the polarization curve and is calculated using equation:

$$R_p = \frac{\Delta V}{\Delta i} \quad (2)$$

where ΔV and Δi represent, respectively, the difference of applied potential on working rebar electrode and corresponsive current density. R_p values were used to calculate the nominal i_{corr} using the Stern–Geary equation:

Table 1
Chemical composition (wt.%) of rebar material.

C	P	S	Mn	Si	Cr	Ni	Mo	Cu	Ti	N_2	Fe
0.43	0.007	0.038	1.11	0.22	0.03	0.11	<0.01	0.37	–	–	Bal.

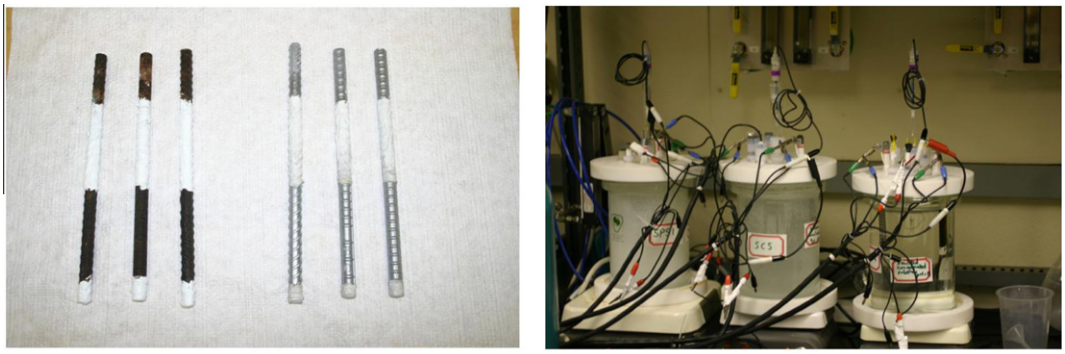

Fig. 1. Test specimens (a) and experimental setup (b).

Table 2
Chemical composition and nominal pH of fresh simulated pore solutions.

Composition	pH	NaOH (g/L)	KOH (g/L)	$Ca(OH)_2$ (g/L)	Na_2CO_3 (g/L)	$NaHCO_3$ (g/L)
SCS	12.6	–	–	2.0	–	–
SPS1	13.3	3.7	10.5	2.0	–	–
SPS4	11.6	0.0833	0.233	–	–	–

$$i_{corr} = \frac{B}{R_p} \quad (3)$$

where B is the Stern–Geary constant, assumed to be 26 mV.

3. Experimental results

3.1. Open circuit potential measurement

Figs. 2 and 3 show the evolution of OCP (sandblasted rebars) with $[Cl^-]$ increment and $[Cl^-]/[OH^-]$ variation in diverse SPSs. Note that the OCP values are the average value of rebar OCP at each $[Cl^-]$ increment step. The solid shapes and the shaded area are the upper and lower boundaries of a dramatic shift in OCP, implying corrosion initiation of rebar at corresponding $[Cl^-]$ range. To be conservative, the $[Cl^-]$ or the $[Cl^-]/[OH^-]$ value at the leftmost boundary of the shaded area, just before an abrupt negative shift in OCP, is considered the threshold value in this study. For all SPSs, prior to reaching the threshold value, the OCP is more positive than −200 mV vs. SCE and the OCP values remain in a relatively stable trend; once the $[Cl^-]$ becomes greater than the threshold value, the OCP shifts negatively by more than 200 mV. The threshold $[Cl^-]$ values show increasing trends with SPS pH increase. Regarding $[Cl^-]/[OH^-]$ threshold values, this trend is not significant for rebars in SCS and SPS1, which may be induced by fewer $[Cl^-]/[OH^-]$ increment steps in SCS solution.

Figs. 4 and 5 exhibit the counterpart functions of Figs. 2 and 3 but for the prerusted bars. Except for the OCP positive shift in the beginning, OCP exhibits a trend of gradual linear decays. The most pronounced decay occurs after the second $[Cl^-]$ addition for all cases. The original OCP positive shift when $[Cl^-]$ increased from

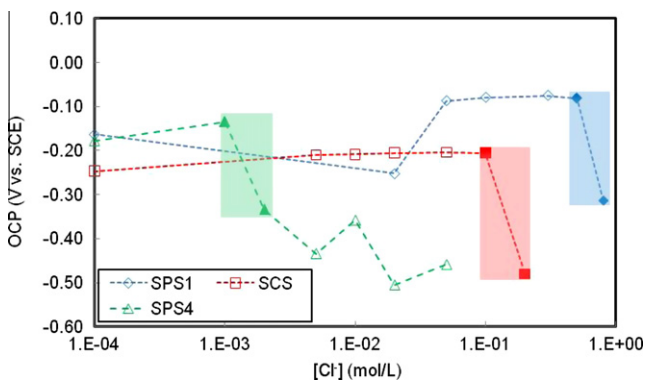

Fig. 2. The evolution of sandblasted rebar OCP with stepwise $[Cl^-]$ increase in diverse SPSs (the solid shapes and the shaded areas are the upper and lower boundary of threshold $[Cl^-]$ range).

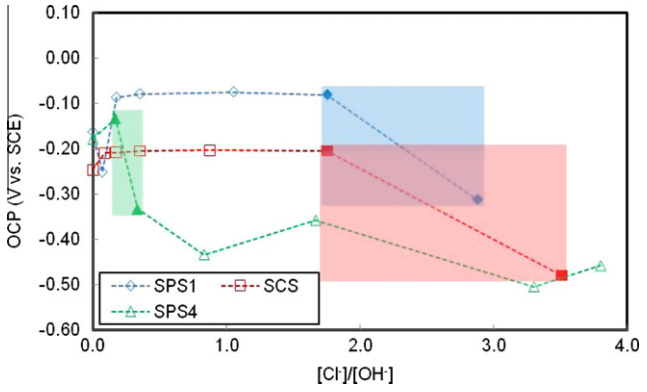

Fig. 3. The evolution of sandblasted rebar OCP as a function of $[Cl^-]/[OH^-]$ variation in diverse SPSs (the solid shapes and the shaded areas are the upper and lower boundary of threshold $[Cl^-]/[OH^-]$ range).

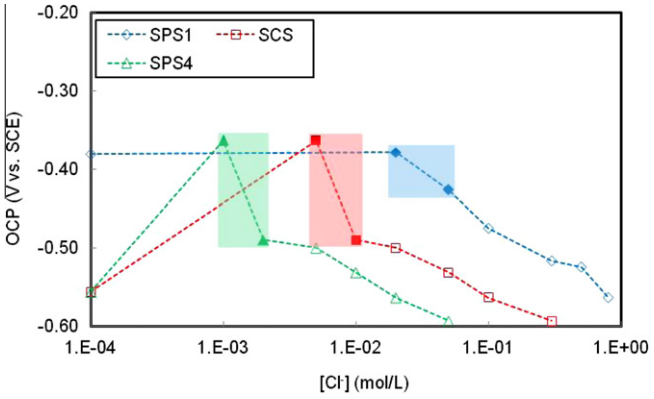

Fig. 4. The evolution of pre-rusted rebar OCP with stepwise [Cl^-] increase in diverse SPSs (the solid shapes and the shaded areas are the upper and lower boundary of threshold [Cl^-] range).

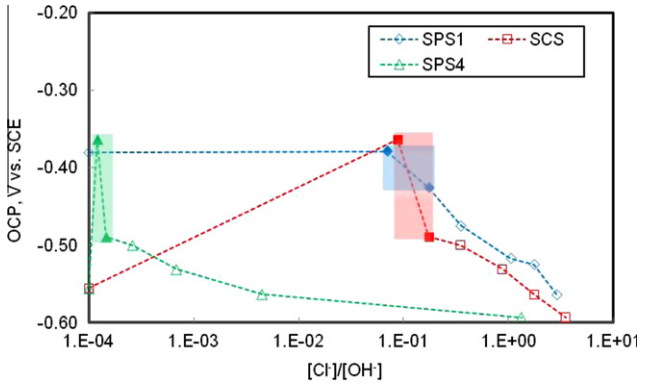

Fig. 5. The evolution of pre-rusted rebar OCP as a function of [Cl^-]/[OH^-] variation in diverse SPSs (the solid shapes and the shaded areas are the upper and lower boundary of threshold [Cl^-]/[OH^-] range).

1×10^{-4} to 1×10^{-3} may be due to the formation of a weak protective layer (a combination of a preformed rust layer and an unstable passive layer), which had not been produced completely. The stable OCP had not been established prior to the first chloride addition. Compared with the results in Figs. 2 and 3, the results from the prerusted rebar (Figs. 4 and 5) revealed the difference of the protective layer between sandblasted and pre-rusted bars. The linear decrement trend is attributed to increasing protective layer breakdown with continuously increasing [Cl^-]. Gradually, the localized corrosion evolved to general corrosion. Like that of sandblasted bars, [Cl^-] threshold values show increasing trends with SPS pH increase. For pre-rusted bar in SPS4 (lower pH solution), the [Cl^-]/[OH^-] threshold level is approximately three orders of magnitude lower that those in SCS and SPS1.

3.2. Linear polarization measurement

Figs. 6 and 7 present the i_{corr} variation of the sandblasted bar as a function of the [Cl^-] stepwise increment and [Cl^-]/[OH^-] variation, respectively, in diverse SPSs. Compared with Figs. 2 and 3, inverse i_{corr} and OCP show abrupt shift trends and the same [Cl^-] and [Cl^-]/[OH^-] threshold determination for SPS4 and SCS. The discrepancy is that the sharp variation of SCS at threshold determination is not so pronounced. Unlike the fluctuation of OCP, the sharp fluctuation of i_{corr} for the sandblasted bar in SPS1 is one step earlier than that of OCP. This means that C_{th}s of the sandblasted bar in SPS1, represented by both [Cl^-] and [Cl^-]/[OH^-], are less than those determined by OCP approaches.

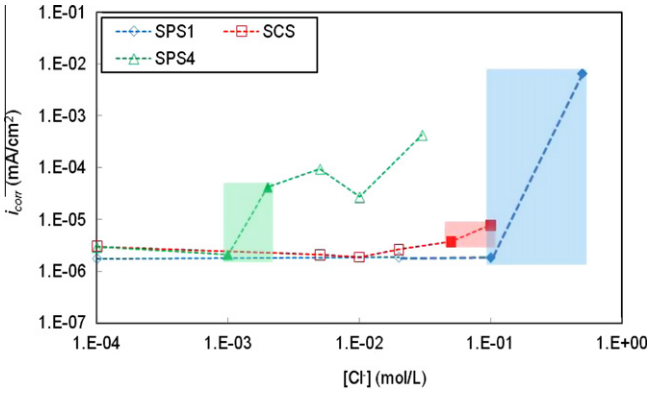

Fig. 6. The evolution of sandblasted rebar i_{corr} with stepwise [Cl^-] increase in diverse SPSs (the solid shapes and the shaded areas are the upper and lower boundary of threshold [Cl^-] range).

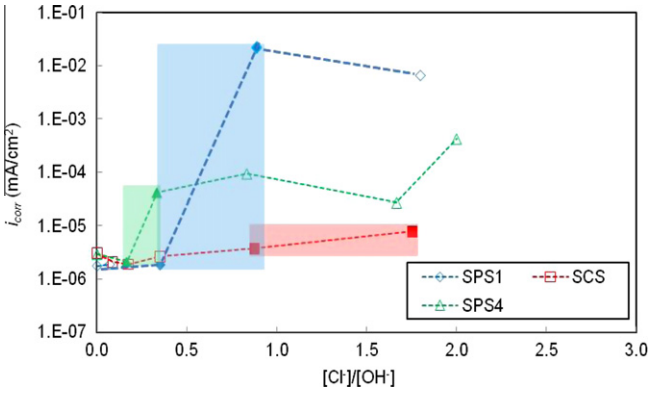

Fig. 7. The evolution of sandblasted rebar i_{corr} as a function of [Cl^-]/[OH^-] variation in SPSs (the solid shapes and the shaded areas are the upper and lower boundary of threshold [Cl^-]/[OH^-] range).

Figs. 8 and 9 show the i_{corr} variation of the prerusted bar as a function of [Cl^-] stepwise increment and [Cl^-]/[OH^-] variation, respectively, in all SPSs. For all SPSs and all stepwise [Cl^-] additions, the fluctuations of i_{corr} are in a range from 1×10^{-5} to 5×10^{-4} mA/cm^2. The sharp fluctuations in these cases are not so apparent. This is because resistance offered by the porous protective layer cannot provide enough corrosion inhibition to polarization current. Therefore, with [Cl^-] stepwise increase, more

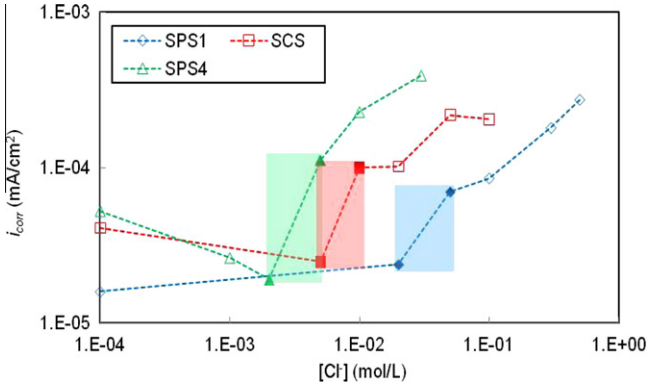

Fig. 8. The evolution of pre-rusted rebar i_{corr} with stepwise [Cl^-] increase in diverse SPSs (the solid shapes and the shaded areas are the upper and lower boundary of threshold [Cl^-] range).

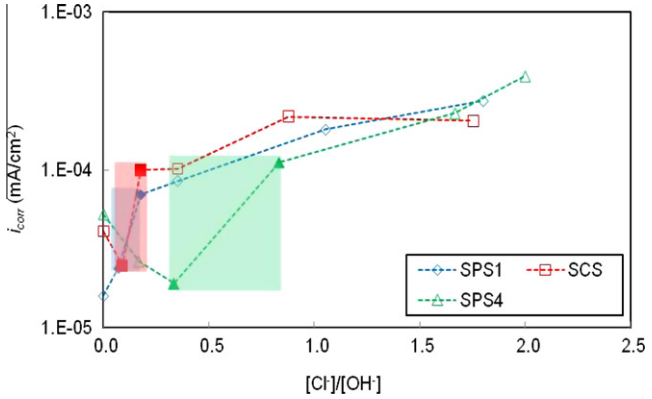

Fig. 9. The evolution of pre-rusted rebar i_{corr} as a function of $[Cl^-]/[OH^-]$ variation in SPSs (the solid shapes and the shaded areas are the upper and lower boundary of threshold $[Cl^-]$ /$[OH^-]$range).

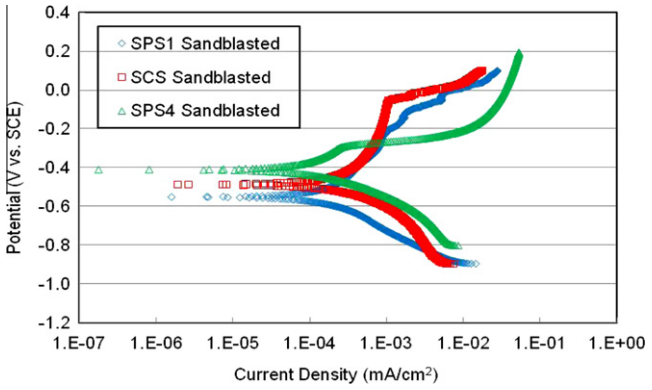

Fig. 10. Potentiodynamic polarization curves of corroded sandblasted bars in chloride-contaminated SPSs.

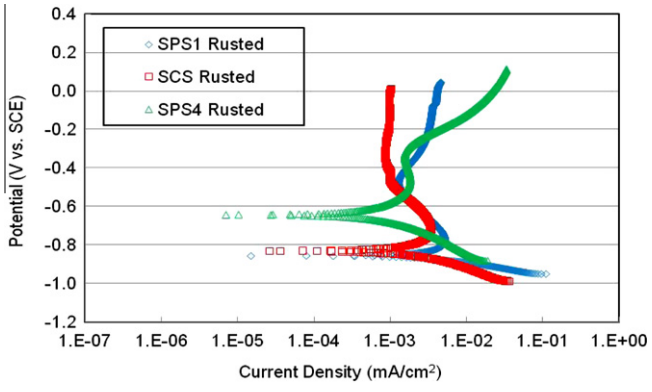

Fig. 11. Potentiodynamic polarization curves of corroded pre-rusted bars in chloride-contaminated SPSs.

active pits appeared and the general corrosion formed. This is similar to the trend shown in Figs. 4 and 5.

3.3. Potentiodynamic polarization measurement

After all rebar corroded according to OCP and LPR criteria, potentiodynamic polarization measurements were conducted for sandblasted and pre-rusted bars. The results are shown in Figs. 10 and 11, respectively. The OCP of both corroded sandblasted and pre-rusted bars moves positively with SPS pH decrease. Interestingly, with less anodic polarization (approximately 200 mV for the sandblasted bar and 100 mV for pre-rusted bar), there is no significant difference of anodic polarization current for both sandblasted and the prerusted bars in three SPS solutions; when polarization is more than 300 mV, both sandblasted and prerusted bars in SPS4 show greater polarization current.

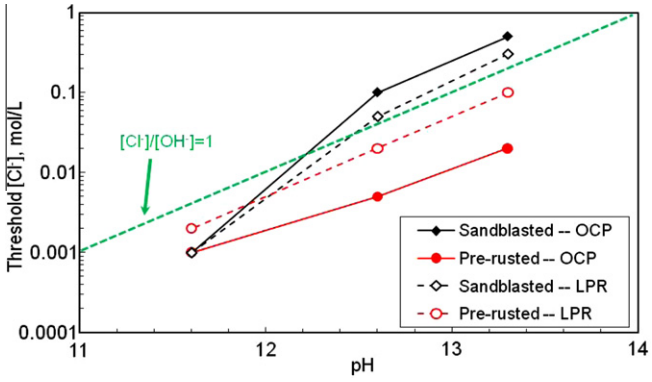

Fig. 12. Plot of threshold $[Cl^-]$ results as function of pH.

4. Discussion

4.1. Chloride threshold level

According to the criterion described in Section 1, when the OCP significantly shifts negatively or the i_{corr} greatly increases, the rebar specimen corrosion is considered to be initiated. The $[Cl^-]$ and $[Cl^-]/[OH^-]$ values acquired from the OCP or i_{corr} before the transilience are considered the threshold values. The threshold $[Cl^-]$ and $[Cl^-]/[OH^-]$ ratios as a function of pH are plotted in Figs. 12 and 13. For comparison purposes, the threshold $[Cl^-]/[OH^-]$ ratio data reported [26] are also plotted in Fig. 13.

Fig. 12 indicates that, at lower pH SPS solution, a trace amount ($\sim 10^{-3}$ mol/L) $[Cl^-]$ can initiate rebar corrosion. This conclusion is consistent regardless of bar surface conditions or the approaches used to determine the C_{th}. When the pH of SPS rises, the threshold $[Cl^-]$ increases for all cases; a similar trend is seen for the threshold $[Cl^-]/[OH^-]$ ratio (in Fig. 13). This indicates that, for high pH SPS (pH > 12.6), a passive film was produced on the rebar surface and gradually improved resistance to chloride attack with pH rising. The threshold $[Cl^-]$ trend lines, acquired from the OCP and LPR criteria, for sandblasted bars are above the $[Cl^-]/[OH^-] = 1$ line when pH was higher than 12.6. However, those for pre-rusted bars are below and parallel to the $[Cl^-]/[OH^-] = 1$ line but are one to three times less. This implies that, with pH increases, corrosion resistance of both sandblast and pre-rusted bars can be improved, and the extent of improvement for sandblasted bars is more pronounced. Regarding adopted electrochemical techniques, close threshold $[Cl^-]$ acquired for the rebars with the same surface condition reveals that both OCP and LPR are sensitive to rebar corrosion initiation in SPSs and applicable for C_{th} determination.

Fig. 13 plots threshold $[Cl^-]/[OH^-]$ as a function of pH. The test results of Li and Sagûës [26] are included for comparison. The results of this study show that, for the sandblasted bar, the similar $[Cl^-]/[OH^-]$ increasing slope for both OCP and LPR threshold determination is similar to the reported trend [26] in high pH range. However, unlike the incremental trends acquired from the reported data, the increasing trends acquired from this study defer to high pH. Nevertheless, the incremental trends at different pH ranges in these two studies confirm a consistent inhibiting effect

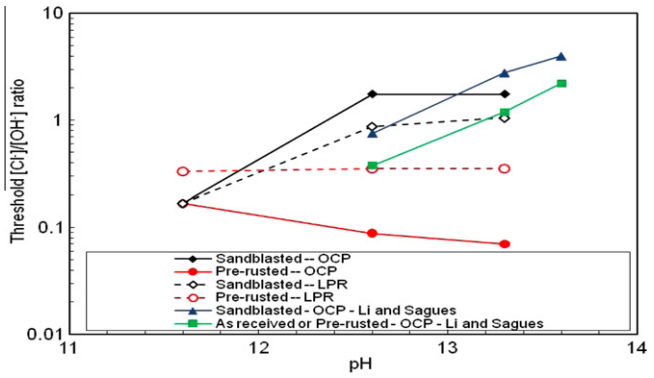

Fig. 13. Plot of threshold $[Cl^-]/[OH^-]$ ratio results and literature data as a function of pH.

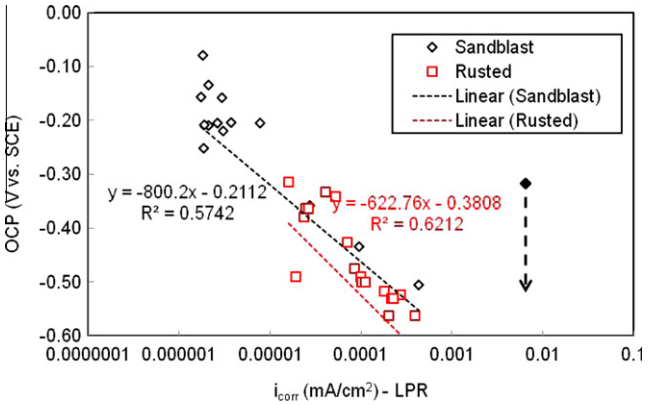

Fig. 14. Rebar OCP as function of i_{corr} (acquired from LPR) for all experimental SPSs.

of OH^- on sandblasted bar corrosion resistance at all concrete pH ranges.

For the prerusted bar, threshold $[Cl^-]/[OH^-]$ ratios are almost identical for the whole experiment pH range for both threshold determination approaches, whereas those acquired from LPR are roughly three times greater than those acquired from OCP. This is not consistent with the reported results [26], which, acquired from the OCP criterion, follow the same increasing slope as that of sandblasted bars. However, the trends acquired in this study are very close to the relationship illustrated in Eq. (1), in which the ratio $[Cl^-]^{0.8}/[OH^-]$ is a constant for rebar corrosion occurrence.

Several causes may result in these different threshold $[Cl^-]/[OH^-]$ trends. The rebars used for Li and Sagûës's [26] study were in the as-received condition (a black mill scale and some red rust spots on the bar surface caused by natural weathering) or prerusted surface (the specimens with mill scale were immersed in agitated, aerated 3.5% NaCl solution for 3 days). After immersing into SPSs, there was still passive film on the rebar surface, but the compactness of the film was compromised by scattered rust spots. Nevertheless, in this study, the pre-rusting process resulted in a bar surface covered with a hard, thick rust layer (shown in Fig. 1a), which makes it difficult to form intact passive film on the rebar surface. Therefore, threshold $[Cl^-]/[OH^-]$ values keep relatively stable with pH of SPS solutions. Another cause may be the fact that the $[Cl^-]$ was adjusted stepwise about every 2 weeks in Li and Sagûës's [26] study, and the chloride concentration was adjusted about every 2 days in the current study. With a longer $[Cl^-]$ adjustment interval, a denser and more compact passive layer can be formed and then result in an increased $[Cl^-]/[OH^-]$ rate. This may also help to explain the discrepant trends of studies for the sandblasted bar in high pH SPS.

4.2. Characteristics of rebar corrosion initiation

Fig. 14 presents rebar OCP as a function of i_{corr} (acquired from LPR) for all experimental SPSs, categorized by sandblasted and pre-rusted bars. Lower i_{corr} (less than 10^{-5} mA/cm^2, which is one order of magnitude less than the corrosion initiation criterion [6]) and a higher OCP (more positive than −250 mV [vs. SCE]) are shown for sandblasted bars when they were in passive status. Greater i_{corr} (far more than 10^{-5} mA/cm^2) and more negative OCP (more negative than −350 mV [vs. SCE)] appear once the rebar was corrosion activated. A decay trend line with slope −800 mV/decade is achieved for the correlation. It is worth noting that the point with very high i_{corr} (~0.01 mA/cm^2) and ~−300 mV (vs. SCE) OCP was achieved when the bar in SPS1 initiated corrosion. The duration for this chloride addition was 1 day, and the OCP kept a negative shift when the experiment was interrupted. For pre-rusted bars, the difference of both OCP and i_{corr} at passive and corrosion active statuses is not so obvious. All OCPs are in the range of −300 to −500 mV and i_{corrs} are in the range of 10^{-5}–5×10^{-4} mA/cm^2. Also, there is a decay trend line with a slope of −622 mV/decade; it is difficult to define the exact OCP or i_{corr} for corrosion occurrence herein. The greater slope of sandblasted bar data represents more pronounced OCP and i_{corr} fluctuation during the course of corrosion occurrence.

The i_{corr}, acquired from LPR in all SPSs, as a function of $[Cl^-]$ and $[Cl^-]/[OH^-]$, respectively, is plotted in Figs. 15 and 16. In both figures, the green dotted line represents the criterion, an averaged sustained corrosion rate higher than 10^{-4} mA/cm^2, for active corrosion. In both plots, before $[Cl^-]$ or $[Cl^-]/[OH^-]$ reaches the threshold value, very low i_{corr}s (less than 10^{-5} mA/cm^2) are exhibited for sandblasted bars. Once the $[Cl^-]$ or $[Cl^-]/[OH^-]$ value is over the threshold value, more than one order of magnitude i_{corr}s are shown. However, for prerusted bars, there is no apparent trend showing corrosion current increase with $[Cl^-]$ or $[Cl^-]/[OH^-]$ abruptly and it indicates that the threshold corrosion rate is not applicable for prerusted rebar. This is because the corrosion of sandblasted bars focused only on the corrosion active pit and a small anodic/big pit and the whole passive surface. Dissimilarly, without an existing dense protective layer, corrosion of prerusted bar occurred on the whole surface (general corrosion). This can also be used to explain the results of potentiodynamic polarization curves. With lower polarization potential, greater polarization current is achieved due to localized corrosion occurrence for both sandblasted and pre-rusted bars in higher pH SPSs; however, further polarization easily facilitates more corrosion active sites produced on rebars in SPS4 (lower pH) and localized corrosion transfers to general corrosion. For the latter case, the polarization

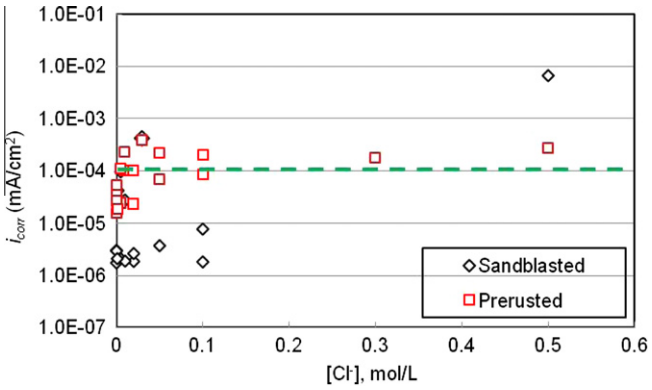

Fig. 15. Corrosion current density as a function of $[Cl^-]$.

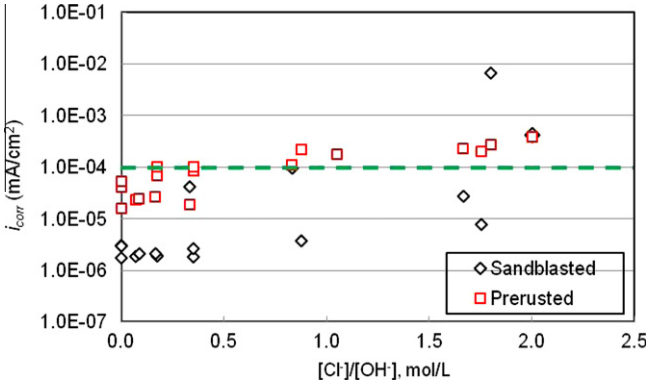

Fig. 16. Corrosion current density as a function of [Cl$^-$]/[OH$^-$].

current of sandblasted and pre-rusted bars in higher pH SPSs is less than that in lower pH SPS.

5. Conclusions

According to experiment results and discussion, the following conclusions can be drawn:

(1) Both [Cl$^-$] and [Cl$^-$]/[OH$^-$] can be used to express C_{th} of a reinforced steel bar in simulated pore solutions. The results of these two threshold expressions, achieved from both OCP and LPR approaches, are in good agreement.
(2) Corrosion resistance of both sandblasted and pre-rusted bars can be improved by raising the pH of SPS solution, implying that [OH$^-$] inhibits rebar corrosion inhibition on the entire SPS solution pH range. The extent of improvement for sandblasted bars is more significant due to the dense protective film produced.
(3) Once initiated, more severe pit corrosion occurs on sandblasted bars, which can be exhibited by more significant OCP and i_{corr} fluctuation. However, there is no direct correlation between [Cl$^-$] or [Cl$^-$]/[OH$^-$] and OCP or i_{corr}.

Acknowledgments

This work was supported by Southwest Research Institute Internal Research and Development Project R8084. Gratitude is due to Robert Carlos and Brian Derby for technical assistance. The authors gratefully acknowledge the technical review of R. Pabalan, programmatic review of E. Pearcy, and assistance of L. Selvey in preparation of this manuscript.

References

[1] Gjørv, Vennesland . Diffusion of chloride ions from seawater into concrete. Cem Concr Res 1979;9(2):229–38.
[2] Yu H, Hartt WH. Effect of reinforcement and coarse aggregates on chloride ingress into concrete and time-to-corrosion: Part I—spatial chloride distribution and implications. Corrosion 2007;63(9):843–50.
[3] Glass GK, Buenfeld NR. The presentation of the chloride threshold level for corrosion of steel in concrete. Corros Sci 1997;39(5):1001–13.
[4] Alonso C, Andrade C, Castellote M. Chloride threshold values to depassivate reinforcing bars embedded in a standardized OPC mortar. Cem Concr Res 2000;30(7):1047–55.
[5] Ann KY, Song HW. Chloride threshold level for corrosion of steel in concrete. Corros Sci 2007;49(11):4113–33.
[6] Angst U, Elsener B, Larsen CK. Critical chloride content in reinforced concrete—a review. Cem Concr Res 2009;39(12):1122–38.
[7] Trejo D, Pillai R. Accelerated chloride threshold testing, Part I—ASTM 615 and A 706 reinforcement. ACI Mater J 2003;100(6):519–27.
[8] Geng Ch, Xu Y, Weng D. A time-saving method to determine the chloride threshold level for depassivation of steel in concrete. Constr Build Mater 2010;24(6):903–9.
[9] Hausmann DA. Steel corrosion in concrete. How does it occur? J Mater Prot 1967:19–23.
[10] Gouda VK. Corrosion and corrosion inhibition of reinforcing steel. Br Corros J 1970;5(2):198–203.
[11] Goni S, Andrade C. Synthetic concrete pore solution chemistry and rebar corrosion rate in the presence of chloride. Cem Concr Res 1990;20:525–39.
[12] Hurley MF, Scully JR. Chloride threshold levels in clad 316L and solid 316LN stainless steel rebar. Corrosion/2002, paper no. 02224. Houston, TX: NACE International; 2002.
[13] Yonezawa T, Ashworth V, Procter RPM. Pore solution composition and chloride effects on the corrosion of steel in concrete. Corrosion 1988;44(7):489–99.
[14] Breit W. Critical chloride content—investigations of steel in alkaline chloride solutions. Mater Corros 1998;49(6):539–50.
[15] Kitowski CJ, Wheat HG. Effect of chlorides on reinforcing steel exposed to simulated concrete solutions. Corrosion 1997;53(3):216–26.
[16] Xu J, Jiang L, Wang J. Influence of detection methods on chloride threshold value for the corrosion of steel reinforcement. Constr Build Mater 2009;23(5):1902–8.
[17] Ueda T, Takewaka K. Performance-based standard specifications for maintenance and repair of concrete structures in Japan. Struct Eng Int 2007;17(4):359–68.
[18] Tritthart J. Chloride binding in cement: II. The influence of the hydroxide concentration in the pore solution of hardened cement paste on chloride binding. Cem Concr Res 1989;19(5):683–91.
[19] Mammoliti LT, Brown LC, Hansson CM. The influence of surface finish of reinforcing steel and pH of the test solution on the chloride threshold concentration for corrosion initiation in synthetic pore solutions. Cem Concr Res 1996;26(4):545–50.
[20] Mohammed TU, Hamada H. Corrosion of steel bars in concrete with various steel surface conditions. ACI Mater J 2006;103(3):233–42.
[21] Manera M, Vennesland Ø, Bertolini L. Chloride threshold for rebar corrosion in concrete with addition of silica fume. Corros Sci 2008;50(2):554–60.
[22] ASTM C876-91: standard test method for half-cell potentials of uncoated reinforcing steel in concrete.
[23] Yu H, Shi X, Hartt WH, Lu B. Laboratory investigation of reinforcement corrosion initiation and chloride threshold content for self-compacting concrete. Cem Concr Res 2010;40(10):1507–16.
[24] Li L, Sagûës AA. Effect of chloride concentration on the pitting and repassivation potentials of reinforcing steel in alkaline solutions. Corrosion/99, paper no. 567. Houston, TX: NACE International; 1999.
[25] Li L, Sagûës AA. Effect of material surface condition on the chloride corrosion threshold of reinforcing steel in alkaline solutions. Corrosion/2000, paper no. 801. Houston, TX: NACE International; 2000.
[26] Li L, Sagûës AA. Chloride corrosion threshold of reinforcing steel in alkaline solutions—open-circuit immersion tests. Corrosion 2001;57(1):19–28.
[27] Li L, Sagûës AA. Chloride corrosion threshold of reinforcing steel in alkaline solutions—cyclic polarization behavior. Corrosion 2002;58(4):305–16.